# MEASUREMENT OF THE SPURIOUS SOUND FIELD GENERATED BY A PARAMETRIC ARRAY LOUDSPEAKER USING EXPONENTIAL SINE SWEEPS

Augusto Fantinelli[1], Marc Arnela[1]

[1] *Human-Environment Research group, La Salle - Universitat Ramon Llull, Catalonia, Spain*

This contribution has been accepted based on the submitted abstract. The submitted manuscript was not reviewed and is reproduced here without edits or corrections by the conference board. Neither the EAA nor the AAA take responsibility for its contents.

Preliminary document

## Abstract

Parametric array loudspeakers use arrays of ultrasonic transducers to generate highly directive audible fields through the non-linear properties of air in the ultrasonic range. They require very high ultrasonic pressure levels to generate the audible field, but these levels, in turn, lead to measurement inaccuracies produced by the microphone. Known as spurious sound, this measurement error can be circumvented by incorporating a filter in front of the microphone to reduce the ultrasonic levels. However, its effects have been studied mainly in the far field and at a few fixed measurement points. This paper explores this phenomenon by mapping the sound field using an automated robotic system, composed of a 6-degree-of-freedom robot mounted on a linear track. By recording exponential sine sweeps and deconvolving with the corresponding inverse filters, sound field maps for the audible and ultrasonic fields are obtained. Measurements were performed with and without the microphone filter to isolate the spurious sound. Results confirm a correlation between the ultrasonic field and the spurious sound, and show that spurious sound levels increase with the audible difference frequency.

**Keywords:** *parametric array loudspeakers, spatial sound-field sampling, exponential sine-sweeps, spurious sound*

## 1. Introduction

Parametric array loudspeakers (PALs) utilise ultrasonic transducers to generate highly directional sound fields [1], [2]. They depend on the nonlinearity of sound propagation in air at ultrasonic frequencies, which causes energy transfer from the ultrasonic to the audible range — i.e., demodulation of the sound. In a sound field composed of two ultrasonic frequencies $f_1$ and $f_2$, this effect causes the generation of a secondary sound field composed by $f_2 + f_1$, the second harmonics of $f_1$ and $f_2$ — which are absorbed by the air — and $f_2 - f_1$, which is called difference-frequency. The difference-frequency can be tuned to be in the audible range, allowing the utilisation of PALs for sound reproduction [3], [4], [5], noise cancelling [6], [7], acoustic identification of materials [8], [9], room acoustics [10], [11] as well as entertainment and informational purposes [12].

The audible sound-field, in turn, is composed by the actual nonlinear difference-frequency field $p_{\mathrm{df}}$ i.e. corresponding directly to $f_2 - f_1$, and a spurious component $p_{\mathrm{ss}}$, caused by receiver nonlinearity [13], [14], [15], proportional to the product of the primary wave amplitudes. When spatially sampling the sound field generated by a PAL, spurious sound affects measured SPLs and must be taken into consideration. This deviation can be especially problematic in the nearfield and at low frequencies, where, despite high primary field levels, the secondary field does not exceed the spurious component, leading to overestimated sound pressure levels.

The most common strategy to mitigate spurious sound is to attenuate the primary-wave pressures using polymer film barriers [14], [16] or resonators [17], [18] to act as filters, but these approaches present practical limitations, such as their frailty and high sensitivity to mounting conditions in the case of the films, and their narrow-band behaviour in the case of the resonators. Acoustic filters based on preprocessing techniques employing phase-cancellation of the primary field also exist [19], [20], but the employment of such techniques affects the frequency response of the PAL device [19]. This paper explores the spurious sound by mapping the response of a flat PAL with 91 transducers in its near and Westerwelt far-fields. A methodology for measuring the ultrasonic and audible fields using ESSs in PALs [10], [21] allows for the correlation

***Corresponding author:*** *marc.arnela@salle.url.edu.*
***Copyright:*** *©2026 Augusto Fantinelli et al. This is an open-access article distributed under the terms of the Creative Commons Attribution 3.0 Unported License, which permits unrestricted use, distribution, and reproduction in any medium, provided the original author and source are credited.*

between the audible range field and the ultrasonic field that generates it for a broad frequency range, and by mapping the sound field with and without an acoustic filter, the spurious sound can be extracted based on the difference between the signals in each position. A robotic arm mounted on a track [22] can be used to obtain the spurious sound pressure in an area in front of the PAL, and the information of the ultrasonic primary pressures and the spurious sound pressures can be used to model the relation between both, allowing for the estimation of the spurious sound directly from the primary sound field amplitudes. Finally, by proposing a model for the relationship between the primary-wave amplitudes and frequencies and the spurious sound, the estimated spurious sound can be deduced from the audible measurements without the filter, allowing simultaneous measurements of the difference-frequency and ultrasonic sound.
The paper is organised as follows. Section 2 presents a review of the spurious sound, and also explains the measurement and calibration techniques. Section 3 presents the sound field mappings, the spurious sound estimation, and the estimation of the difference-frequency sound from the combination sound and ultrasonic range measurements for an audible field of 1 kHz. Finally, Section 4 provides the conclusions.

## 2. Methodology

### 2.1. The Parametric Array effect and the spurious sound

The parametric acoustic array (PAA) effect is the phenomenon whereby audible frequencies corresponding to the difference frequency between two ultrasound tones are generated by non-linearities in the propagation of sound in air when the primary ultrasonic waves have sufficient energy. A sound field composed of two ultrasonic frequencies $f_1$ and $f_2$ of sufficient amplitude causes the generation of a secondary sound field composed by the sum of their individual frequencies ($f_2 + f_1$), the second harmonics of $f_1$ and $f_2$, which are frequencies so high they get promptly absorbed by the air, and $f_2 - f_1$, which is called difference-frequency and can be adjusted to be audible.
To trigger the above non-linearities, the primary (ultrasonic) tones must have very high amplitudes, which affect the measured values in two ways. One is the radiation pressure or pseudo-sound generated by the incidence of these wavefronts on the transducer [13], [14], [16], and the other is non-linearities in the electronics of the microphone cartridge [13], [14], [16]. Both are usually assessed simultaneously as spurious sound or detector non-linearity, although it is known that the pseudo-sound contributes little to the inaccuracies in comparison to electric non-linearities on the microphone's pre-amplifier [14].
In practical terms, the spurious sound $p_{\mathrm{ss}}$ manifests itself as an increment in the measured sound pressure $p_{\mathrm{m}}$, meaning measured values correspond to [14]

$$p_{\mathrm{m}} = p_{\mathrm{df}} + p_{\mathrm{ss}}, \tag{1}$$

with $p_{\mathrm{df}}$ being the difference frequency pressure produced in the audible field. The relative effect of the spurious sound reduces with increasing frequency, since the PAA effect becomes stronger and the levels corresponding to the difference-frequency become higher, and with the decay of the primary levels due to distancing from the source.
Typically, the spurious sound $p_{\mathrm{ss}}$ is modelled as

$$p_{\mathrm{ss}} = K\, p_{\mathrm{u1}}\, p_{\mathrm{u2}}, \tag{2}$$

where $p_{\mathrm{u1}}$ and $p_{\mathrm{u2}}$ are the amplitudes of the ultrasonic waves in the primary field [14], [18], [20], and there's no explicit frequency dependence. We call $p_{\mathrm{u1}}\, p_{\mathrm{u2}}$ cross-frequency product. Existing literature regarding the spurious sound is dedicated to determining the $K$ coefficient in the far field of the PAL through simulated or experimental data [14], [15], [20], usually considering that $K$ is constant in frequency — usually a result from averaging $K$ and ignoring the frequency dependence — and looking for a function of the axial distance from the source. We propose a different approach, relating the isolated spurious sound, calculated from measurements with and without a polymeric filter, and the measured amplitude of the primary waves directly, in an aperture of 1 m × 2 m. The proposed model for the relation between spurious sound and the cross-frequency product is

$$p_{\mathrm{ss}}(f_{\mathrm{df}}) = K\, p_{\mathrm{u1}}\, p_{\mathrm{u2}} + N\, f_{\mathrm{df}}, \tag{3}$$

where, besides the $K$ coefficient, there's an $N$ term that weights the frequency dependence.

### 2.2. Experimental setup

Measurements were performed in the anechoic chamber of La Salle - Universitat Ramon Llull, using two GRAS 46BF-1 1/4" microphones. One was covered with a layer of matte acetate tape (commonly referred to as "magic tape") to measure the audible field without the spurious sound effect [23], and another was used without the protection grid to measure the ultrasonic field. The microphones with and without the acetate tape can be seen on the top row of Figure 1.
The analysed PAL had 91 Multicomp Pro MCUST16A40S12RO transducers, arranged in 9 concentric rings plus one central transducer. The radius of the radiation area of the prototype is $a = 98$ mm. To characterise the PAL, we set the sweep's lowest frequency $f_{\mathrm{i}} = 20$ Hz and its highest frequency $f_{\mathrm{i}} = 14$ kHz and use a total duration of $T = 1$ s, adding also 1 s of silence before and after the sweep. A linear fade-in from 20 Hz to 80 Hz and fade-out from 12 kHz to 14 kHz are applied to avoid pre-ringing artefacts [24]. This paper will

Preliminary document

limit itself to analysing only the 4 kHz frequency and its corresponding ultrasonic frequency, 45.4 kHz. The emitted signals were acquired using a Type 3160-A-022 Brüel & Kjaer LANXI module with a UA-3102-041 front end. The signals were amplified using an Ecler XPA3000 amplifier with its gain set to achieve a peak voltage of 17 V. Following [11], an equalisation of the amplifier was done to compensate for the change in waveform and maintain the excitation voltage constant.

Each microphone was mounted on the automated robotic measurement system described in [22], to scan an area of 1 m in the radial direction and 2 m in the axial direction.The scan resolution was 10 mm over the first 500 mm of the axial direction to better visualise the vicinity of the PAL, and 40 mm in the remaining area. In total, 6278 positions were measured over 35 h per scan. A picture of the setup, including the PAL, the microphone, and the automated system, is shown in the bottom row of Figure 1.

**Figure 1:** Top row: 1/4" microphone without grid (left) and with acetate tape (right). Bottom row: experimental setup, with UR5 robot and the analysed PAL.

## 3. Results

### 3.1. Pressure maps at the ultrasonic range

Figure 2 shows the results in the ultrasonic range: (a) pressure field of the second primary wave $p_{\mathrm{u2}}$ at 45.4 kHz ($f_c + 4$ kHz), and (b) pressure field of the first primary wave $p_{\mathrm{u1}}$ at the carrier frequency $f_c = 41.4$ kHz, and (c) the cross-frequency product $p_{\mathrm{u2}} p_{\mathrm{u1}}$. Looking first at Figure 2a, observe that the generated ultrasonic field consists of a high directive beam with high SPLs, surrounded by weaker sidelobes. The plot also displays comb filtering, characteristic of constructive and destructive interferences between the individual transducers. An interesting remark can be made about the spatial distribution of the ultrasonic pressure at the carrier frequency. Comparing Figures 2a and 2b, the mapping of the PAL at the carrier frequency has the same aspect as the ultrasonic frequency that corresponds to 45 kHz. This can be an indication that the directivity of the transducer is practically constant with the frequency in this range, and the changes in the audible range are resulting from the PAA effect being more efficient and better cross-frequency coupling between transducers [25].

### 3.2. Pressure maps in the audible range

Figure 3 displays the mapped SPLs at 4 kHz, measured with and without the acoustic filter in front of the microphone. The combination sound measured without the presence of the acetate film, and thus contaminated with spurious sound, is displayed in Figure 3a, whereas results with the film and this without spurious sound are shown in Figure 3b.

The sound field is composed of a beam with a peak SPL between 40 mm and 250 mm, aligned with the transducer's axial direction. In the beam region, the sound radiates like a plane wave, evident by the non-decaying nature of the sound field as we get further from the source in the axial direction. However, the audible SPL in the immediate vicinity of the PAL remains small, and the plane wave forms only after the local maxima are surpassed in the ultrasonic range. Figure 3c displays the SPL maps for the isolated spurious sound. Remarkably, the spurious sound seems directly proportional to the product of the primary waves shown in Figure 2. Furthermore, observe that the levels of the spurious sound are larger than those of the audible difference frequency sound in the very near-field of the PAL and along the beam.

### 3.3. Spurious sound estimation

As explained in Section 2, the spurious sound is proportional to the product of the primary waves $p_{\mathrm{u1}}\ p_{\mathrm{u2}}$. Figure 4a represents the pressure values of the spurious sound $p_{\mathrm{ss}}$ against this product. To facilitate their location in space, values are coloured according to the radial direction of the PAL, with yellow corresponding to the radiation axis, red to positive $+x$, and blue to negative $-x$. The values in Figure 4a are then used to fit a regression line, and from there, the coefficients of $K$ and $N$ in Eq. (3) are determined. The figure includes also, for comparison, the classical estimation of the spurious sound, where $p_{\mathrm{ss}}$ is set to be proportional to $p_{\mathrm{u1}}\, p_{\mathrm{u2}}$, see Eq. (2). The values of $K$ and $N$ at 4 kHz are $K = 1.0574\mathrm{e}{-04}\ \mathrm{Pa}^{-1}$ and $N = 7.40\mathrm{e} - 02\ \mathrm{Pa\,Hz}^{-1}$.

Observe in the figure how, while the classic method overestimates the spurious sound levels at a certain $p_{\mathrm{u1}}\, p_{\mathrm{u2}}$ level, the $1^{st}$ order model presents a good fit with the measured spurious sound. The plateau that forms at lower values of $p_{\mathrm{u1}}\, p_{\mathrm{u2}}$ can be explained by that region not presenting high enough levels of $p_{\mathrm{u1}}\, p_{\mathrm{u2}}$. Since the primary waves do not have enough energy to generate any relevant difference-frequency

Preliminary document

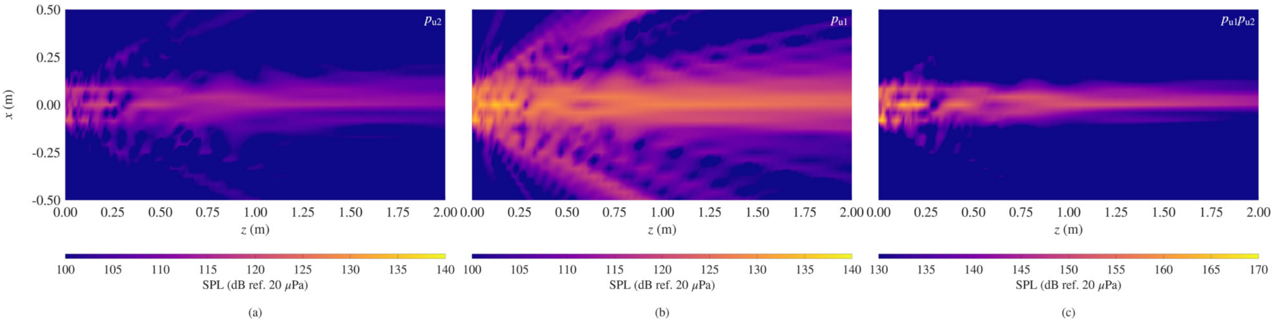


**Figure 2:** SPL mappings of the ultrasonic tones and radiation pressure generated by the flat PAL. (a) $p_{u2}$ (45.4 kHz), (b) $p_{u1}$ (41.4 kHz), (c) $p_{u1}p_{u2}$.

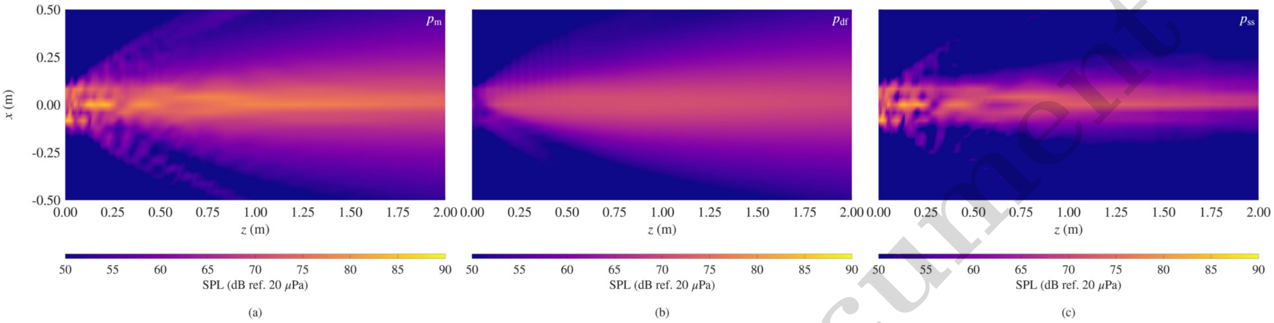


**Figure 3:** SPL mappings of the measured combination audio (without the film), the difference frequency audio (with the film), and isolated spurious sound generated by the flat PAL at 4 kHz. (a) $p_m$, (b) $p_{df}$, (c) $p_{ss}$.

Preliminary document

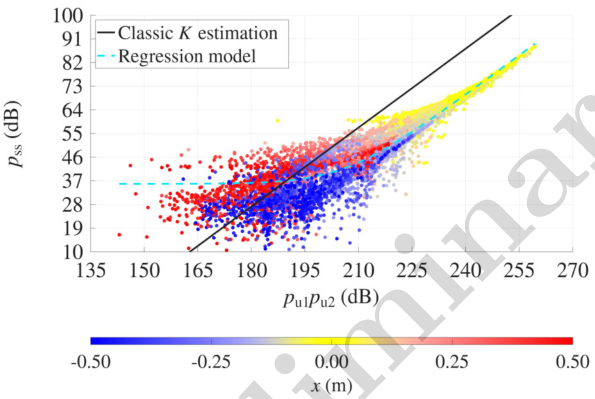


**Figure 4:** Scatter plot of each measured position, relating the cross-frequency product $p_{u1}\,p_{u2}$ and the spurious sound $p_{ss}$ .

or spurious sound levels, that region is dominated by background noise. The classic estimation does not represent this behaviour. Another aspect that can be highlighted is that relevant values of spurious sound, i.e., of an order of magnitude comparable to the difference-frequency sound at a given frequency, occur only when the cross-frequency product is very large, as consistently observed over the section of the beam (yellow-coloured points). Evidently, points directly in front of the PAL will receive higher $p_{u1}\,p_{u2}$, which potentiates the PAA effect in the audible field.

### 3.4. Removing spurious sound

Finally, an attempt is made to remove the spurious sound from a measurement performed without a filter in front of the microphone. The spurious sound is estimated from the ultrasonic primary waves using the expression in Eq. (3), and the values of $K$ and $N$ derived above. Figure 5a shows the estimated spurious sound, and Figure 5b shows the reconstructed audible field without this measurement error. As can be observed, Figure 5a displays the same shape as Figure 3c. The same can be said when comparing Figure 5b with Figure 3b, in the case of the difference-frequency sound. It is worth noting that the reconstruction appears more accurate in the Westerwelt far-field, which can be explained by the sound pressure being nearly constant with increasing distance compared to the near-field.

## 4. Conclusions

This work aimed to explore the spurious sound of a parametric array loudspeaker in its near-field and Westerwelt far-field regions by mapping them using an automated robotic system equipped with a microphone. The spurious sound was isolated by subtracting the audible difference-frequency sound, and the combination of the difference-frequency and spurious sound was measured with and without an acoustic filter, respectively. It was found that previous models for the relationship between the spurious sound and the primary-wave pressures overestimate the spurious sound values outside the far-field, and

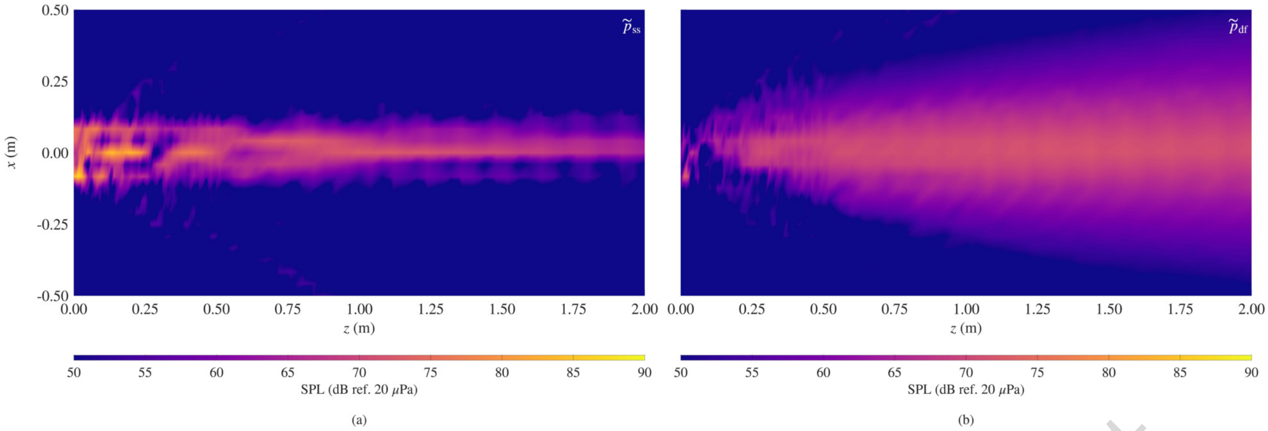


**Figure 5:** SPL mappings of the reconstructed audible sound pressures. (a) Reconstructed spurious sound $\tilde{p}_{ss}$ (b). Estimated difference-frequency sound $\tilde{p}_{df}$ .

that a dependence on the difference-frequency must be accounted for. A model that also considers the audible frequency was proposed, enabling the estimation of spurious sound at different spatial positions and the recovery of difference-frequency levels at 4 kHz, yielding accurate results.

Future work involves scaling this analysis to broadband, thereby enabling analysis of spurious sound at varying difference frequencies. Since the difference-frequency audio and spurious sound are separable, post-processing techniques can also be further developed for application in this context. In a theoretical sense, although a relationship between the spurious sound, the primary ultrasonic waves, and the difference-frequency levels was assessed, the influence of certain design choices, such as transducer size, spacing, and distribution shape, has yet to be addressed.

## 5. Acknowledgments

This publication is part of the project CharPAL PID2025-175028NB-I00 funded by MICIU/AEI/10.13039/501100011033 and by ERDF, EU. The authors thank the Catalan Government (Departament de Recerca i Universitats) for the grant 2021 SGR 01396 awarded to the HER group.

## References

[1] F. J. J. Pompei, “Sound from ultrasound, The parametric array as an audible sound source,” Ph.D. dissertation, Massachusetts Institute of Technology, 2002.

[2] J. Zhong, R. Kirby, and X. Qiu, “The near field, westervelt far field, and inverse-law far field of the audio sound generated by parametric array loudspeakers,” *J. Acoust. Soc. Am.*, vol. 149, no. 3, pp. 1524–1535, 2021.

[3] Y. Zhu, W. Ma, Z. Kuang, M. Wu, and J. Yang, “Optimal audio beam pattern synthesis for an enhanced parametric array loudspeaker,” *J. Acoust. Soc. Am.*, vol. 154, no. 5, pp. 3210–3222, 2023.

[4] M. Li, T. Zhuang, K. Chen, J.-X. Zhong, and J. Lu, “Deep learning-based approach for identification and compensation of nonlinear distortions in parametric array loudspeakers,” *IEEE Signal Processing Letters*, 2025.

[5] J.-X. Zhong, J. Ji, X. Xia, H. Heo, and Y. Jing, “Audible enclaves crafted by nonlinear self-bending ultrasonic beams,” *Proceedings of the National Academy of Sciences*, vol. 122, no. 12, e2408975122, 2025.

[6] N. Tanaka and M. Tanaka, “Active noise control using a steerable parametric array loudspeaker,” *J. Acoust. Soc. Am.*, vol. 127, no. 6, pp. 3526–3537, 2010.

[7] N. Tanaka and M. Tanaka, “Mathematically trivial control of sound using a parametric beam focusing source,” *J. Acoust. Soc. Am.*, vol. 129, no. 1, pp. 165–172, 2011.

[8] A. Sugahara, H. Lee, S. Sakamoto, and S. Takeoka, “Measurements of acoustic impedance of porous materials using a parametric loudspeaker with phononic crystals and phase-cancellation method,” *Appl. Acoust.*, vol. 152, pp. 54–62, 2019.

[9] M. Arnela, E. Vidaña-Vila, A. Fantinelli, A. Moñux-Bernal, J. Vaquerizo-Serrano, and J. C. Socoró, “Generation of ultrasonic and audible sound waves for the automatic classification of packaging waste in reverse vending machines,” *Waste Management*, vol. 204, p. 114 934, 2025.

[10] M. Arnela, C. Martínez-Suquía, and O. Guasch, “Characterization of an omnidirectional parametric loudspeaker with exponential sine sweeps,” *Appl. Acoust.*, vol. 182, p. 108 268, 2021.

Preliminary document

[11] M. Arnela, R. Burbano-Escolà, R. S. Ribeiro, and O. Guasch, “Reverberation time and random-incidence sound absorption measured in the audible and ultrasonic ranges with an omnidirectional parametric loudspeaker,” *Appl. Acoust.*, vol. 229, p. 110 414, 2025.

[12] Holosonics, *Audio spotlight directional speakers*, , https://www.holosonics.com/applications. Last accessed 2025-04-07.

[13] M. B. Bennett and D. T. Blackstock, “Parametric array in air,” *J. Acoust. Soc. Am.*, vol. 57, no. 3, pp. 562–568, 1975. DOI: https://doi.org/10.1121/1.380484. [Online]. Available: https://pubs.aip.org/asa/jasa/article-abstract/57/3/562/681464/Parametric-array-in-air?redirectedFrom=fulltext.

[14] I. O. Wygant et al., “50 khz capacitive micromachined ultrasonic transducers for generation of highly directional sound with parametric arrays,” *IEEE Transactions on Ultrasonics, Ferroelectrics, and Frequency Control,*, vol. 56, no. 1, pp. 193–203, 2009. DOI: https://doi.org/10.1109/TUFFC.2009.1019.

[15] P. Ji, W. Liu, S. Wua, J. Yang, and W.-S. Gan, “An alternative method to measure the on-axis difference-frequency sound in a parametric loudspeaker without using an acoustic filter,” *Appl. Acoust.*, vol. 73, pp. 1244–1250, 2012. DOI: http://dx.doi.org/10.1016/j.apacoust.2012.04.010.

[16] M. Toda, “New type of acoustic filter using periodic polymer layers for measuring audio signal components excited by amplitude-modulated high-intensity ultrasonic waves,” *J. Audio Eng. Soc.*, vol. 53, no. 10, pp. 930–941, 2005. DOI: https://doi.org/10.3390/s21227470.

[17] W. Kim, B. Oh, J. Rho, and W. Moon, “An accurate measurement of parametric array using a spurious sound filter topologically equivalent to a half-wavelength resonator,” *Applied Acoustics*, vol. 240, p. 110 910, 2025. DOI: https://doi.org/10.1016/j.apacoust.2025.110910.

[18] C. Ye, Z. Kuang, M. Wu, and J. Yang, “Development of an acoustic filter for parametric loudspeaker in air,” *Japanese Journal of Applied Physics*, vol. 50, 2011. DOI: https://doi.org/10.1143/JJAP.50.07HE18.

[19] T. Kamakura, S. Sakai, H. Nomura, and M. Akiyama, “Parametric audible sounds by phase-cancellation excitation of primary waves,” in *Proc. of Acoustics ’08*, Acoustical Society of America and European Acoustics Association, 2008, pp. 7993–7998.

[20] P. Ji and J. Yang, “An experimental investigation about parameters’ effects on spurious sound in parametric loudspeaker,” *Appl. Acoust.*, vol. 565, pp. 67–74, 2019. DOI: https://doi.org/10.1016/j.apacoust.2018.12.015.

[21] M. Arnela, C. Martínez-Suquía, and O. Guasch, “Carrier frequency influence on the audible and ultrasonic fields generated by an omnidirectional parametric loudspeaker excited with exponential sine sweeps,” *Appl. Acoust.*, vol. 200, p. 109 073, 2022.

[22] A. Fantinelli, M. Arnela, E. Brandão, and E. Fernandez-Grande, “A robotic system for space-time characterization of parametric acoustic sound sources,” in *Proc. of Forum Acusticum 2025*, European Acoustics Assosciation, Málaga, Spain, 2025.

[23] J. Zhong et al., “Low frequency audio sound field generated by a focusing parametric array loudspeaker,” *IEEE/ACM Transactions on Audio, Speech, and Language Processing*, vol. 30, pp. 3098–3109, 2022.

[24] I. Bork, “Exponential sweep check using Hilbert transform,” *Acta Acust. united Ac.*, vol. 100, no. 4, pp. 659–666, 2014.

[25] T. Zhuang, J.-X. Zhong, G. Ma, F. Niu, and J. Lu, “Modeling a phased array of parametric array loudspeakers using the spherical wave expansion,” *IEEE Transactions on Audio, Speech and Language Processing*, vol. 33, pp. 309–318, 2025. DOI: 10.1109/TASLPRO.2024.3522764.

Preliminary document